

Article

Experimental Study on Sulfur Deactivation and Regeneration of Ni-Based Catalyst in Dry Reforming of Biogas

Rei-Yu Chein ^{1,*} , Yen-Chung Chen ² and Wei-Hsin Chen ^{3,4,5,*} ¹ Department of Mechanical Engineering, National Chung Hsing University, Taichung 40227, Taiwan² Thin Film Engineering Department, Taiwan Semiconductor Manufacturing Co., Tainan 74144, Taiwan; pigs7654@gmail.com³ Department of Aeronautics and Astronautics, National Cheng Kung University, Tainan 70101, Taiwan⁴ Research Center for Smart Sustainable Circular Economy, Tunghai University, Taichung 40704, Taiwan⁵ Department of Mechanical Engineering, National Chin-Yi University of Technology, Taichung 41170, Taiwan

* Correspondence: rychein@dragon.nchu.edu.tw (R.-Y.C.); chenwh@mail.ncku.edu.tw (W.-H.C.);

Tel.: +886-4-22840433 (R.-Y.C.); +886-6-2004456 (W.-H.C.)

Abstract: The dry reforming of methane (DRM) using biogas and a Ni-based catalyst for syngas production was studied experimentally in this study under the presence of H₂S. Using the nonpoisoned DRM performance as a comparison basis, it was found that the catalyst deactivation by the sulfur chemisorption onto the catalyst surface depends on both reaction temperature and time. With low reaction temperatures, a complete sulfur coverage was resulted and could not be regenerated. With higher reaction temperatures, the H₂S coverage decreased, and the poisoned catalysts could be regenerated. The experimental results also indicated that a catalyst deactivation could not be avoided by using the bi-reforming of methane by adding O₂ or H₂O simultaneously in the reactant due to the stronger chemisorption capability of sulfur. The catalyst could only be regenerated after it was poisoned. The experimental results indicated that the high-temperature oxidation process was the most effective process for regenerating the poisoned catalyst.

Keywords: dry reforming of methane; biogas; catalyst poison; and catalyst regeneration



Citation: Chein, R.-Y.; Chen, Y.-C.; Chen, W.-H. Experimental Study on Sulfur Deactivation and Regeneration of Ni-Based Catalyst in Dry Reforming of Biogas. *Catalysts* **2021**, *11*, 777. <https://doi.org/10.3390/catal11070777>

Academic Editor: Stefano Cimino

Received: 15 May 2021

Accepted: 23 June 2021

Published: 26 June 2021

Publisher's Note: MDPI stays neutral with regard to jurisdictional claims in published maps and institutional affiliations.



Copyright: © 2021 by the authors. Licensee MDPI, Basel, Switzerland. This article is an open access article distributed under the terms and conditions of the Creative Commons Attribution (CC BY) license (<https://creativecommons.org/licenses/by/4.0/>).

1. Introduction

Energy shortage and environmental pollution are issues related to the sustainable development of human beings. With the continuous consumption of fossil energy sources, renewable energy has attracted wide attention for development and utilization. Moreover, the development of environmentally friendly energy utilization technologies for the traditional energy conversion processes also receives much attention. Biogas is one of the renewable biomass energies. The utilization of biogas is recognized as true carbon neutral. Due to the negative costs regarding the reduction of disposable wastes, the utilization of biogas as an energy source has both financial and environmental benefits [1].

Biogas is mainly composed of CH₄ and CO₂. Depending on the feedstock, CH₄ amount varies from 45 to 75%, while CO₂ accounts for 20~55% [2]. In addition to CH₄ and CO₂, biogas also contains a small amount of oxygen, nitrogen, sulfide, and ammonia [3]. At present, biogas is mainly used as fuel for power generation [4]. The CH₄ is used as the energy source, while the CO₂ lowers the heating value of biogas. Biogas-based power generation is a well-developed and commercialized technology [5].

Alternatively, biogas can also be used for synthetic gas (syngas) production in which the CH₄ and CO₂ are reformed into H₂ and CO [6–8]. The traditional CH₄-based syngas production technologies are steam reforms of methane (SRM) [9], partial oxidation of methane (POM), and dry reforming of methane (DRM) [10]. The biogas can be used as the feedstock for these technologies [6–8]. In SRM or POM, a steam or oxygen addition is required. In DRM, CH₄ is reformed with CO₂. The CO₂ contained in biogas can be

used directly in DRM. As compared with SRM and POM, the syngas production from DRM using biogas as a feedstock has several advantages. Since CO₂ is one of the main gas species in biogas, there is no need for CO₂ separation and sequestration. To enhance the DRM performance, the captured CO₂ can be utilized in the biogas-based DRM for syngas production. The syngas produced by DRM has the H₂/CO ratio of 1, which is suitable for liquid fuel synthesis from Fischer-Tropsch synthesis [11].

Although DRM is of great significance from both a renewable energy usage and environmental protection point of view, it is not ready in practical applications due to at least two problems [12]. One of the main problems is the high energy consumption because DRM is an endothermic reaction. To maintain a high conversion rate, there must be a high energy input. Another major problem of DRM is catalyst deactivation. It has been shown that catalyst deactivation is mainly caused by high-temperature active metal sintering and carbon deposition [13]. The catalyst deactivation results in a reduction in reaction conversion rate and increased catalyst renewal cost.

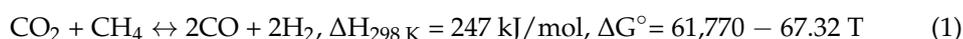
In addition to the problems of energy consumption and catalyst deactivation, the effect of impurities contained in actual biogas for DRM is also a key issue for syngas production. Due to its low cost and high activity, Ni-based catalysts have been widely adopted in the CH₄-based reforming reaction [14]. During biogas production, it inevitably produces H₂S, and its removal is necessary for various biogas applications. Similar to coal gasification and SRM, the presence of H₂S, even with a small amount, will cause the catalyst poison in DRM [15,16]. In general, the catalyst poison mechanism is that the H₂S reacts with the active metal to occupy the active site of the catalyst, which, in turn, leads to catalyst deactivation [17]. In the actual reaction process, the catalyst poison is affected by many factors such as reaction temperature, gas composition, reactor parameters, H₂S concentration, and type of catalyst [13,18].

The catalyst poisoned by H₂S has been studied extensively in SRM [19]. As compared with SRM, studies on the H₂S effect on DRM performance are relatively few. In this study, a detailed experimental study was carried out to examine the catalyst poison by H₂S in DRM. To reduce the cost of DRM, the regeneration of poisoned catalysts is necessary [18]. Poisoned catalyst regeneration via conventional methods and its performance were also reported in this study.

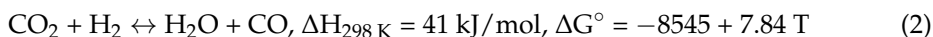
2. Thermodynamic Background

2.1. Dry Reforming of Biogas

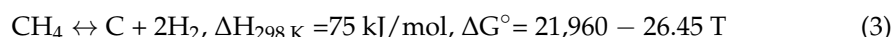
The overall dry reforming of biogas consists of four reversible reactions, which are [20] the dry reforming of methane (DRM):



reverse water-gas shift (RWGS) reaction [21]:



methane decomposition (MD):



Boudouard reaction:



DRM is a highly endothermic reaction and is favored at high temperatures and low pressures. With the coexistence of CH₄, CO₂, H₂, and CO, several side reactions are possible. Equations (3) and (4) are two main side reactions related to carbon formation during the reaction. In Equations (1)–(4), the standard free energy changes ΔG° are also shown. By setting ΔG° = 0, the upper or lower limit temperatures for reactions to occur

can be obtained. From Equations (1)–(4), the lower limit temperatures for the endothermic DRM, RWGS, and MD reactions to occur are 640 °C, 820 °C, and 557 °C, respectively. The upper limit temperature for an exothermic BR reaction is 700 °C. In the temperature range of 557–700 °C, carbon will be formed from methane cracking or the Boudouard reaction.

With the presence of H₂S in DRM, several chemical reactions are possible. The reaction between H₂S and CO₂ [16,22] is



This reaction is thermodynamically favorable at relatively high temperatures. In principle, the formation of COS is also possible [22]:



2.2. Sulfur Chemisorption on Nickel

According to the study by Rostrup-Nielsen and Christiansen [17], the loss of activity of Ni-based catalysts through sulfur compounds can be due to strong sulfur chemisorption on the nickel surface, which prevents the further adsorption of reactant molecules. The reaction of sulfur chemisorption on Ni can be expressed as



It has been pointed out by Rostrup-Nielsen [17,23] and Bartholomew [24] that the fractional surface coverage depends on the value of partial pressure ratio of $p_{\text{H}_2\text{S}}/p_{\text{H}_2}$. Besides, the formation of Ni–S also is influenced by the reaction temperature, gas-phase composition, and reactor parameters. Since the sulfur chemisorption process is theoretically reversible and exothermal, surface Ni–S can be regenerated by stopping H₂S feeding or by temperature enhancement.

3. Experimental

Figure 1 shows the test setup of the experiment. The reactant consists of CH₄, CO₂, and N₂. After mixing in the mixing chamber, the reactant is sent to a tubular quartz reactor in which the catalyst is filled. The reactor's diameter is 4 mm. The reactor is placed horizontally in a temperature-controllable furnace. After the reaction, the product is sent to the condenser at which the produced H₂O in the product is condensed. The dried product is sent to the GC for analyzing the molar flow rate of each species contained in the dried product. In this study, N₂ is regarded as an inert gas, and its flow rate is used as the basis for computing the flow rate of other gas species in the product. As shown in Figure 1, there are two N₂ supplies: one is H₂S-free N₂, while the other one is H₂S-contained N₂. To study the H₂S effect in DRM, H₂S-contained N₂ is used.

For the poisoned catalyst regeneration, the O₂ and steam treatments are to be employed. To reduce the cost of the experiment, the O₂ contained in the air is used in the O₂ treatment for the catalyst regeneration. As shown in Figure 1, the air is supplied from the air tank. In the steam treatment for catalyst regeneration, an HPLC pump is used to supply the liquid water. After preheating, the water vapor is mixed with dried reactant, as stated above.

Based on our previous studies [15,25], the good catalytic ability and thermal stability of DRM can be resulted by using the Ni-Ce/Al₂O₃ catalysts. To focus on the effect of the H₂S-poisoned DRM performance, 20 wt%Ni-5 wt%CeO₂/Al₂O₃ was adopted in this study. Detailed preparation and characterization of the catalyst can be found in our previous studies [15,25]. More detailed characterizations for the catalysts before and after use, such as TEM, TGA, and XPS, have been reported extensively in the literature [18,26–28].

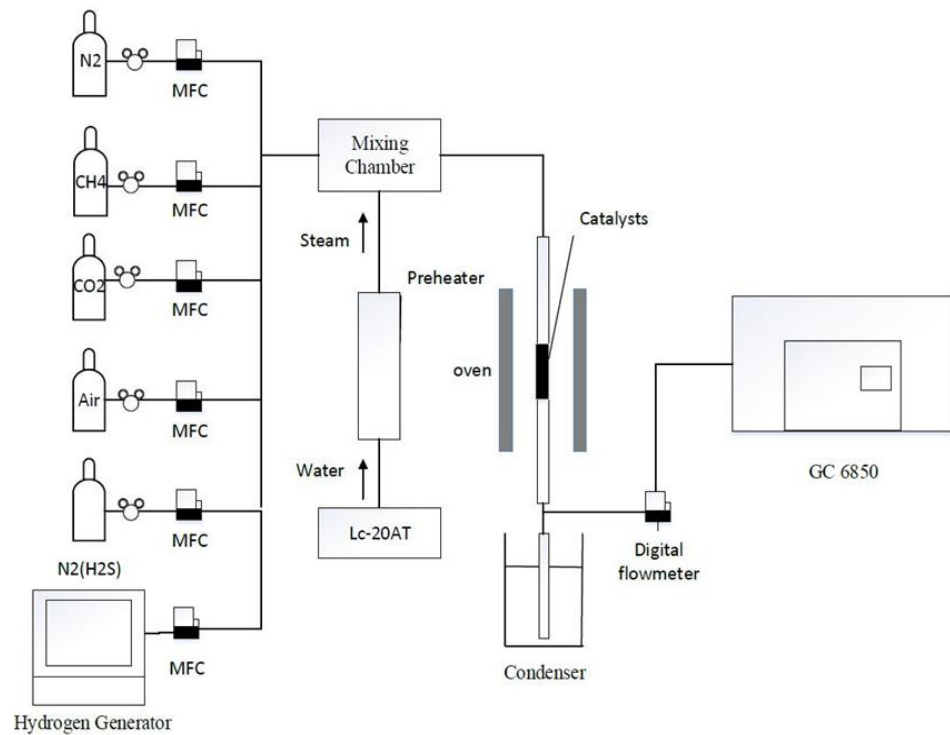


Figure 1. A schematic of the experimental setup.

The DRM performance is characterized by the following performance indices:

$$\text{CH}_4 \text{ conversion : } X_{\text{CH}_4} = \frac{F_{\text{CH}_4,\text{in}} - F_{\text{CH}_4,\text{out}}}{F_{\text{CH}_4,\text{in}}} \times 100\% \quad (8)$$

$$\text{CO}_2 \text{ conversion : } X_{\text{CO}_2} = \frac{F_{\text{CO}_2,\text{in}} - F_{\text{CO}_2,\text{out}}}{F_{\text{CO}_2,\text{in}}} \times 100\% \quad (9)$$

$$\text{H}_2 \text{ yield : } Y_{\text{H}_2} = \frac{F_{\text{H}_2,\text{out}}}{F_{\text{CH}_4,\text{in}}} \quad (10)$$

$$\text{CO yield : } Y_{\text{CO}} = \frac{F_{\text{CO},\text{out}}}{F_{\text{CH}_4,\text{in}}} \quad (11)$$

$$\text{H}_2/\text{CO ratio : } \text{H}_2/\text{CO} = \frac{Y_{\text{H}_2}}{Y_{\text{CO}}} \quad (12)$$

In these equations, $F_{i,\text{in}}$ and $F_{i,\text{out}}$ ($i = \text{CH}_4, \text{CO}_2, \text{H}_2, \text{CO}$) are the molar flow rate of species i at the reactor inlet and outlet, respectively. It is noted that the H_2 and CO yields are based on the feed CH_4 molar flow rate. For the stoichiometric DRM reaction, the stoichiometric yield of H_2 and CO (syngas) is 2, while the H_2/CO ratio is 1.

4. Results and Discussion

4.1. Experimental Parameters

Based on the thermodynamic background described above, the reaction temperature T is chosen in the range of 700–900 °C, and the reaction pressure is fixed as 1 atm. The weight of the filled catalyst is fixed as 0.5 mg. This results in a volume of the catalyst bed of 0.033 mm³. The total volume flow rate of the reactant is fixed as 50 standard cubic centimeters per minute (sccm), and the detailed composition of the reactant is shown in Table 1. For the $\text{CH}_4/\text{CO}_2 = 1/1$ case, it corresponds to a stoichiometric DRM reaction. For $\text{CH}_4/\text{CO}_2 = 1/2$, it corresponds to the excess CO_2 supply for the DRM reaction. In the $\text{CH}_4/\text{CO}_2 = 1/0.5$ case, it corresponds to the lean CO_2 supply for the DRM reaction. Moreover, this also corresponds to the typical components in the biogas [8].

Table 1. Composition of simulated biogas used in the experiment.

Case	Molar Ratio	CH ₄ (sccm)	CO ₂ (sccm)	N ₂ (sccm)
1	CH ₄ /CO ₂ = 1/0.5	15	7.5	27.5
2	CH ₄ /CO ₂ = 1/1	15	15	20
3	CH ₄ /CO ₂ = 1/2	15	30	5

The poisoning effect is always correlated with the H₂S concentration contained in the reactant. Based on the studies by Ashrafi et al. [26] and Yang [27], the magnitude of the H₂S concentration contained in the reactant affects the speed of the stabilization of the catalyst activity, and the phenomenon of catalyst deactivation is similar for different H₂S concentrations. Based on these studies, a single H₂S concentration with a value of 100 ppm was chosen in this study.

4.2. DRM without H₂S

Figure 2 shows the effect of reaction temperature on the DRM performance without the H₂S effect for the CH₄/CO₂ = 1/1 case. The experimental data shown in Figure 2 were taken when the reaction temperature reached the designated value, and the data collection lasted for 18 h. For every 15 min, the data from the experiment were reported. Due to endothermic reaction, it can be seen that the DRM performance is enhanced as the reaction temperature increases. The thermally stable results of the CH₄ conversion, CO₂ conversion, H₂ yield, and CO yield, as shown in Figure 2a–d, can be obtained when the reaction time increases for T = 800 and 900 °C. For T = 700 °C, a slight decrease in the DRM performance can be found. Since there is no H₂S effect, the decrease in the DRM performance is mainly due to the catalyst deactivation from the carbon deposition. By comparing the CH₄ and CO₂ conversions shown in Figure 2a,b, one can see that CO₂ conversion is higher than the CH₄ conversion for the three reaction temperatures studied. From the theoretical background, this is apparently due to the contribution from RWGS in which CO₂ reacted with H₂ to form CO and H₂O. In Figure 2c,d, the H₂ and CO yields are shown. The variations of the H₂ and CO yields are similar to those of X_{CH₄} and X_{CO₂}. Additionally, based on the thermodynamic background, the theoretical maximum yields of H₂ and CO would be 2. As shown in Figure 2c,d, the yields of H₂ and CO exceed 2 slightly for the T = 900 °C case due to the uncertainty of the experimental measurements. From the theoretical background, the H₂/CO ratio has a value of unity. Figure 2e shows the H₂/CO ratio based on the results shown in Figure 2c,d. H₂/CO is less than unified due to the consumption of H₂ and the formation of CO in the RWGS reaction. As noted above, the DRM reaction is the dominant reaction at high reaction temperatures. The H₂ and CO yields follow the similar variation trend of X_{CH₄}. In the following discussions, only X_{CH₄} and X_{CO₂} are reported.

Using the data from 15 to 18 h shown in Figure 2a,b, the averaged conversions of CH₄ and CO₂ can be obtained and listed in Table 2. As shown in Table 2, the experimental results of the present study agree well with those reported in the literature [29–31].

Table 2. Comparison between the present study and data reported in the literature without H₂S poison. CH₄/CO₂ = 1/1.

Temperature	Present Study		Ref [29]		Ref [30]		Ref [31]	
	X _{CH₄}	X _{CO₂}						
700 °C	55%	68%	53%	68%	53%	64%	56%	70%
800 °C	78%	91%	82%	88%	80%	85%	80%	89%
900 °C	88%	96%	N/A	N/A	N/A	N/A	94%	98%

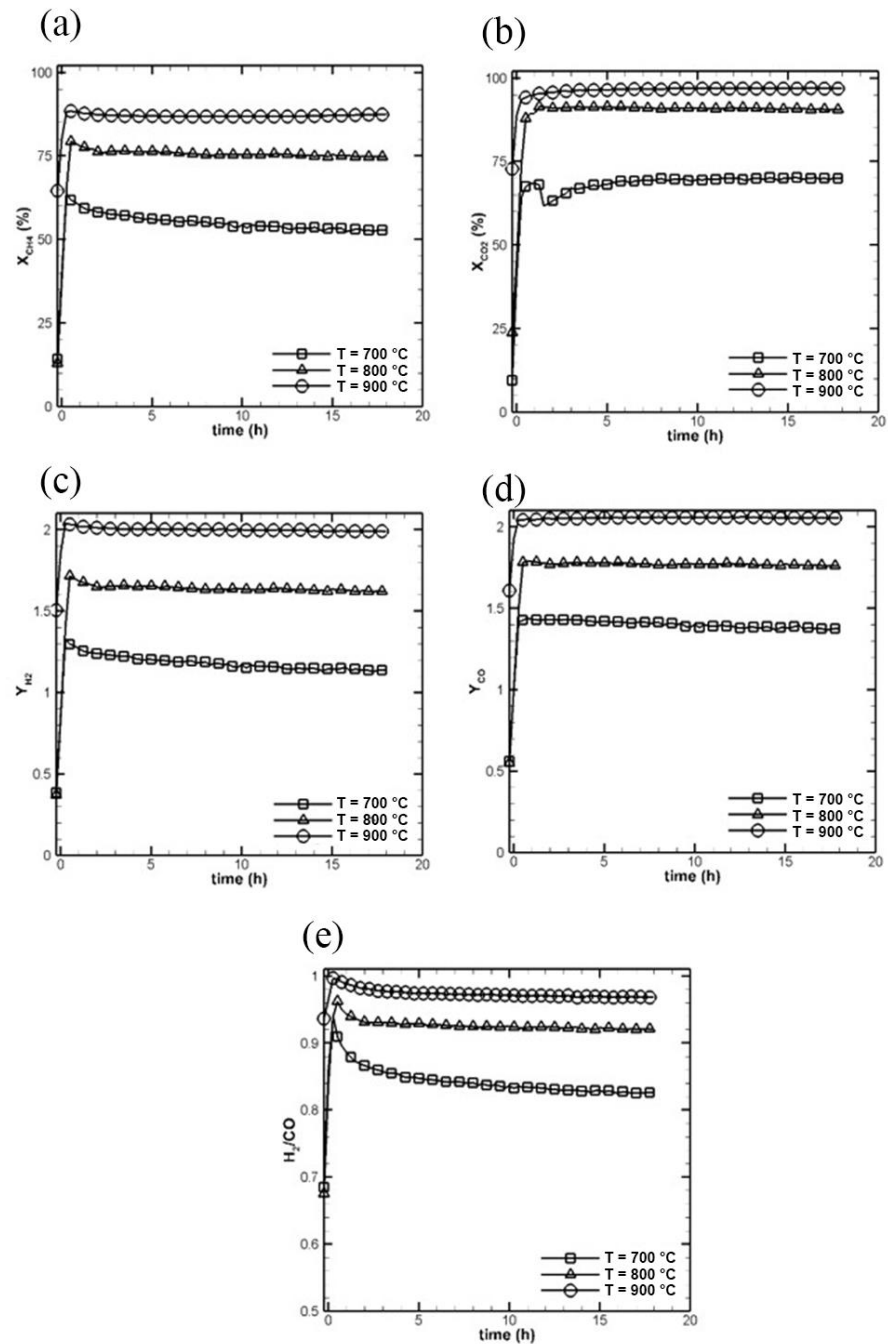


Figure 2. Effect of the reaction temperature on the DRM performance without a H_2S presence in the reactant. $\text{CO}_2/\text{CH}_4 = 1$. (a) CH_4 conversion, (b) CO_2 conversion, (c) H_2 yield, (d) CO yield, and (e) H_2/CO ratio.

4.3. DRM with H_2S

From the results shown in Figure 2, the DRM reaction is the dominant reaction at high reaction temperatures. The H_2 and CO yields follow the similar variation trend of X_{CH_4} . In the following discussions, only X_{CH_4} and X_{CO_2} are reported. In Figure 3, the effect of H_2S on the DRM performance is shown for three reaction temperatures. The test procedure and reactant used are the same as those for Figure 2, except that the H_2S is introduced in the reactant. This is achieved by switching the H_2S -free N_2 flow to a H_2S -contained N_2 flow. It is seen that the catalyst activity is decreased as the H_2S is introduced in the reactant. From Figure 3, it is also clearly seen that the catalyst poisoned by H_2S depends on the reaction temperature and reaction time. For $T = 700$ °C, linear decreases in both X_{CH_4}

and X_{CO_2} are obtained as the reaction time increases, as shown in Figure 3a,b, respectively. For $T = 800\text{ }^\circ\text{C}$, slight decreases in X_{CH_4} and X_{CO_2} resulted in an earlier reaction time. As the reaction time is greater than 4 h, exponential decays in both X_{CH_4} and X_{CO_2} result. As the reaction time is greater than 12 h, both X_{CH_4} and X_{CO_2} approach steady-state values, indicating that the sulfur coverage on the catalyst surface reaches a saturated condition. For $T = 900\text{ }^\circ\text{C}$, the catalyst poisoned by H_2S is to a smaller extent as compared with $T = 700\text{ }^\circ\text{C}$ and $800\text{ }^\circ\text{C}$ under the same reaction time. That is, the sulfur coverage decreases with the increased reaction temperatures. It is also expected that the sulfur coverage on the catalyst surface will reach a saturated condition when the test time is increased.

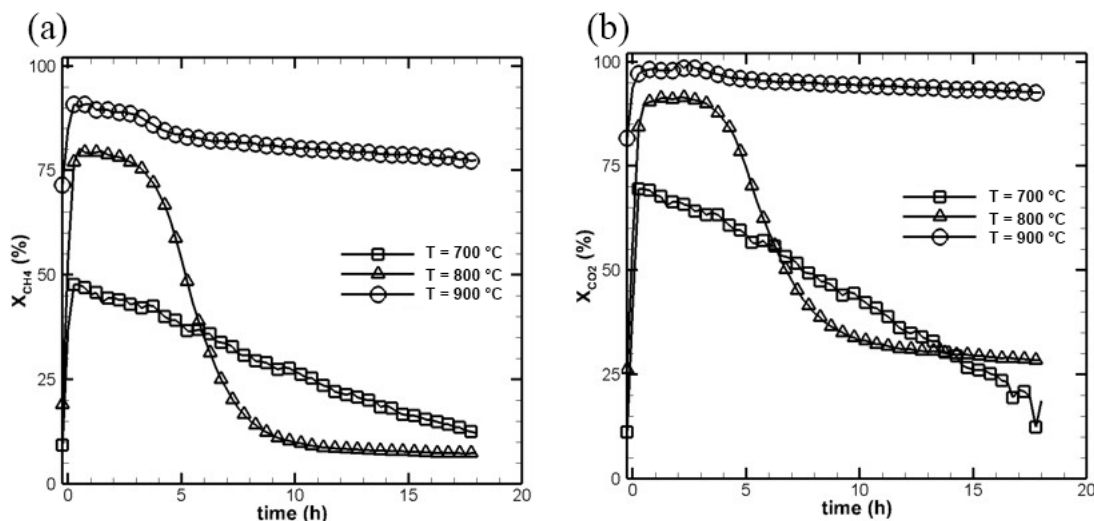


Figure 3. Effect of the reaction temperature on the DRM performance with a H_2S presence in the reactant. $CO_2/CH_4 = 1$. (a) CH_4 conversion and (b) CO_2 conversion $^\circ\text{C}$.

From Figure 3, it is seen that the rate of the poison of Ni catalyst depended on both the reaction temperature and reaction time. For $T = 700\text{ }^\circ\text{C}$, the catalyst activity lost immediately and exhibited a constant rate. From the variation trend, it was expected that zero X_{CH_4} and X_{CO_2} would be reached for a longer reaction time. For $T = 800\text{ }^\circ\text{C}$ and $900\text{ }^\circ\text{C}$, the rate of poison was about the same for the first 4 h of the reaction time. After that, it was seen that the rate of poison dropped exponentially for the $T = 800\text{ }^\circ\text{C}$ case, while a constant rate of poison was found for $T = 900\text{ }^\circ\text{C}$. In the study of the catalyst performance for SRM by Appari et al. [32] and Yang [27], an exponential decay of catalyst activity was also found for reaction temperatures in the $700\text{--}900\text{ }^\circ\text{C}$ range for the SRM case. The results shown in Figure 3 agree with those reported by Appari et al. [32] and Yang [27] for the $T = 800\text{ }^\circ\text{C}$ case. The above results were related to the sulfur chemisorption ability on Ni catalysts under different reaction temperatures. As pointed out by many studies [16,33,34], it is therefore suggested that higher reaction temperature is preferred in DRM when H_2S -contained biogas is used as the feedstock.

In Figure 4, the effect of the CO_2 amount on the H_2S -poisoned DRM performance is shown for reaction temperature $T = 800\text{ }^\circ\text{C}$. For the higher CO_2 amount case, i.e., $CH_4/CO_2 = 1/2$, the DRM performance follows the same trend as the $CH_4/CO_2 = 1/1$ case discussed above. From the thermodynamic analysis, carbon formulation can be enhanced by reducing the CO_2 amount in the DRM [35,36]. For the $CH_4/CO_2 = 1/0.5$ case, due to more carbon formulations, it can be seen that the variation trend of X_{CH_4} is different from the $CH_4/CO_2 = 1/1$ and $1/2$ cases. It is seen that CH_4 conversion drops immediately in the early reaction time and then reaches a steady-state value. As compared with the $CH_4/CO_2 = 1/1$ and $1/2$ cases, the initial drop in X_{CH_4} is due to catalyst deactivation caused by both carbon deposition and sulfur poison. It is noted that the X_{CH_4} can be enhanced by increasing the CH_4/CO_2 ratio for both the non-poisoned and poisoned catalysts shown in Figure 4a.

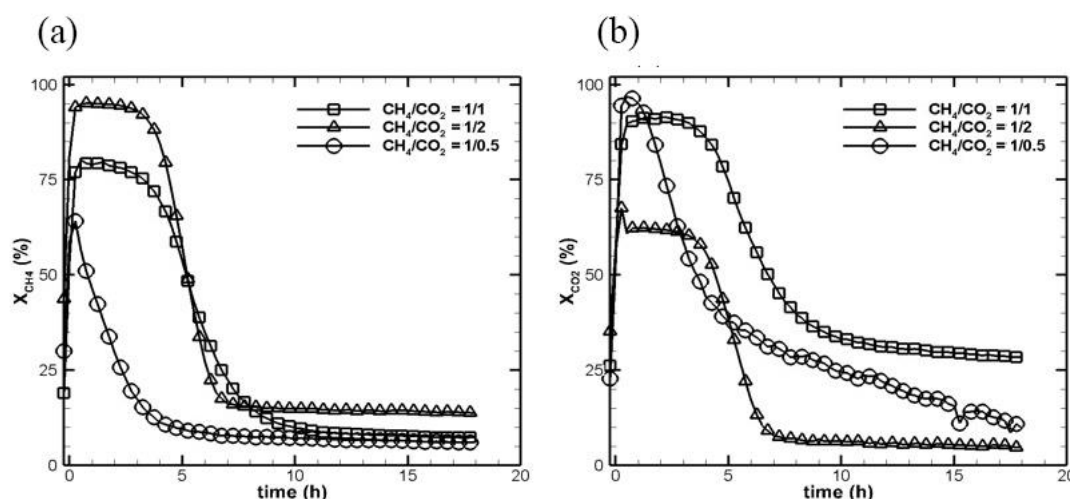


Figure 4. Effect of the CH₄/CO₂ ratio on the DRM performance with the presence of H₂S in the reactant. T = 800 °C. (a) CH₄ conversion and (b) CO₂ conversion.

In Figure 4b, the effect of the CH₄/CO₂ ratio on X_{CO₂} during the catalyst poison is shown. It is interesting to note that, for the CH₄/CO₂ = 1/0.5 case, X_{CO₂} was found to continuously decrease after an immediate drop when test time increases. As mentioned above, this variation is related to catalyst deactivation due to both the carbon deposition and sulfur poison. With an increased CH₄/CO₂ ratio, a lower X_{CO₂} was obtained due to the excess CO₂ supply in the reaction. Based on the results shown in Figure 4b, this applies to both poisoned and nonpoisoned catalysts.

By comparing the results shown in Figures 2–4, it can be realized that a quick catalyst deactivation is dominated by sulfur poison. The same conclusion was also made in the study by Appai et al. [32]. Moreover, the Ce contained in the catalyst enhances the capability of carbon deposition resistance. Therefore, the effect of carbon deposition on catalyst deactivation would be to a lesser extent as compared with the sulfur poison. Further support of this conclusion can be made in the discussion on the poisoned catalyst regeneration using high temperatures.

4.4. Bi-Reforming of Methane with H₂S

Since H₂S chemisorption onto the catalyst surface is a reversible process, surface-adsorbed sulfur can be removed. High-temperature, O₂ oxidation, and steam treatments are conventional methods used to regenerate the sulfur-poisoned reforming catalyst. Based on these regeneration technologies, it would also be interesting to examine the catalyst activity as the reactant contains O₂ or steam, in addition to H₂S. With O₂ or steam added to the reactant, the reaction system becomes a bi-reforming of methane [37,38]. For the O₂ addition case, the partial oxidation of methane (POM) or complete oxidation of methane (COM), depending on the O₂ amount added, along with DRM, may occur simultaneously during the reaction. The stoichiometric POM and COM are written as

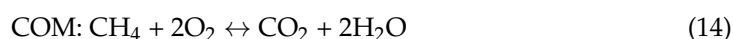


Figure 5 shows the effect of a O₂ addition on DRM with and without H₂S poison at T = 800 °C. As mentioned in the experimental setup, the O₂ supply is from the air, and the volume flow rate ratio of the reactant is CH₄/CO₂/O₂ = 15/15/2 (sccm). For the nonpoisoned catalyst case, the O₂ addition can enhance the X_{CH₄}, as shown in Figure 5a, but lowers the X_{CO₂}, as shown in Figure 5b, due to the CO₂ production from POM or COM. For the poisoned catalyst case, the catalyst activity loss can still be found with a O₂ addition in the reactant for reaction times greater than 5 h. This implies that the chemisorption of

H₂S onto catalyst activity sites is stronger than the catalytic reaction between CH₄ and O₂. The DRM performance can only be improved when the coverage of H₂S reaches a saturated condition.

The effect of a H₂O addition on the DRM performance with and without H₂S poison at T = 800 °C is shown in Figure 6. The volumetric flow rate ratio of the reactant is CH₄/CO₂/H₂O = 15/15/10 (scm). With the H₂O addition, the steam reforming of methane (SRM), along with DRM, may occur simultaneously during the reaction. The stoichiometric SRM is written as

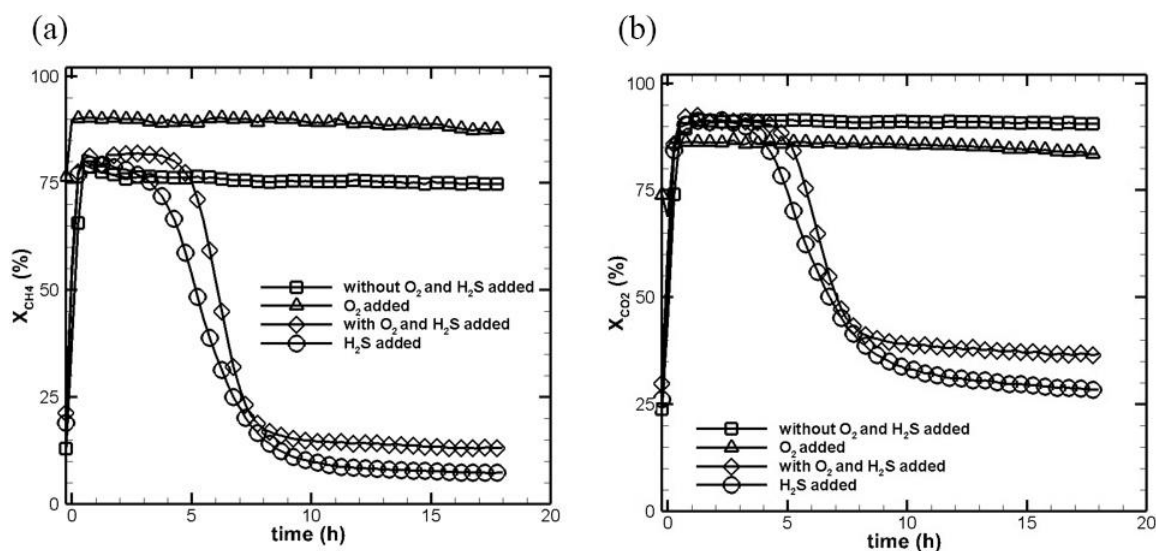


Figure 5. Effect of O₂ addition on the DRM performance. T = 800 °C. (a) CH₄ conversion and (b) CO₂ conversion.

For the nonpoisoned case, it can be seen that the H₂O addition can enhance the X_{CH₄} due to SRM, as shown in Figure 6a. However, due to the H₂O addition, the water–gas shift reaction is also enhanced and results in a lower X_{CO₂} due to more CO₂ production, as shown in Figure 6b. Similar to the O₂ addition, the H₂S poison is the dominant reaction, and the catalyst activity loss is still found for the H₂O addition, as shown in Figure 6. The DRM performance can only be improved when the coverage of sulfur reaches a saturated condition.

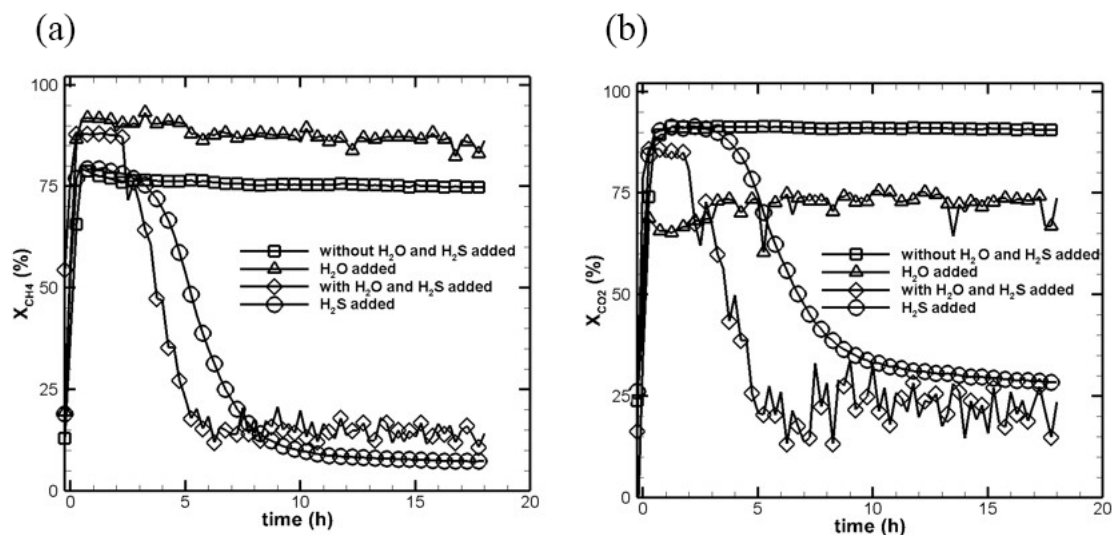


Figure 6. Effect of the H₂O addition on the DRM performance. T = 800 °C. (a) CH₄ conversion and (b) CO₂ conversion.

4.5. Catalyst Regeneration

From the results shown in Figures 5 and 6, it can be concluded that the simultaneous addition of O₂ or H₂O in the DRM cannot avoid the catalyst deactivation due to the stronger chemisorption of sulfur onto the catalyst as compared to O₂ or H₂O. Therefore, catalyst regeneration can only be carried out after the catalyst has been poisoned. To regenerate this sulfur-poisoned reforming catalyst, three different regeneration methods were adopted in this study, including the high-temperature sulfur-free treatment, high-temperature oxidation treatment, and high-temperature steam treatment, as listed in Table 3 [32,39]. The poisoned catalyst regeneration under the high-temperature sulfur-free treatment is shown in Figure 7 for various reaction temperatures. The poison experiment was performed for the first 8 h. After that, the H₂S-contained N₂ gas was switched to H₂S-free N₂ gas, and the measurements lasted for 10 h. As shown in Figure 7a,b, the catalyst activity recovery depends on the reaction temperature. For the T = 700 °C case, the catalyst activity cannot be regenerated. As pointed out by many studies [26,40], the regenerating reaction is irreversible when the reaction is below 700 °C. For the T = 800 °C and 900 °C cases, the catalyst activity can be regenerated. With the increasing reaction time, it can be expected that the catalyst activity can approach the H₂S-free performance, as listed in Table 2. The results shown in Figure 7 demonstrate that sulfur poison is the dominant factor causing catalyst deactivation, as mentioned above. In the study by Izquierdo et al. [18], the tri-reforming of biogas using a Ni-based catalyst was studied. From the TGA analysis, they identified that the carbon deposition amount onto the catalyst was low. From the quick catalyst deactivation, they made the conclusion that the catalyst deactivation was mainly due to sulfur poison.

Table 3. Details of the poisoned catalyst regeneration treatments.

Regeneration	Detail Conditions
High-temperature reaction	T = 700~900 °C. The catalyst was poisoned from 0 to 7 h, followed by a H ₂ S-free DRM test for 8 h.
high-temperature steam	T = 800 °C. The catalyst was poisoned from 0 to 12 h, regenerated by 10 sccm steam from 12 to 14 h to form NiO, reduced NiO to Ni by 20 sccm H ₂ from 14 to 16 h, and DRM-tested using regenerated catalyst from 16 to 33 h.
High-temperature oxidation	T = 800 °C. The catalyst was poisoned from 0 to 12 h, regenerated by 10 sccm air from 12 to 14 h to form NiO, reduced NiO to Ni by 20 sccm H ₂ from 14 to 16 h, and DRM test using regenerated catalyst from 16 to 33 h.

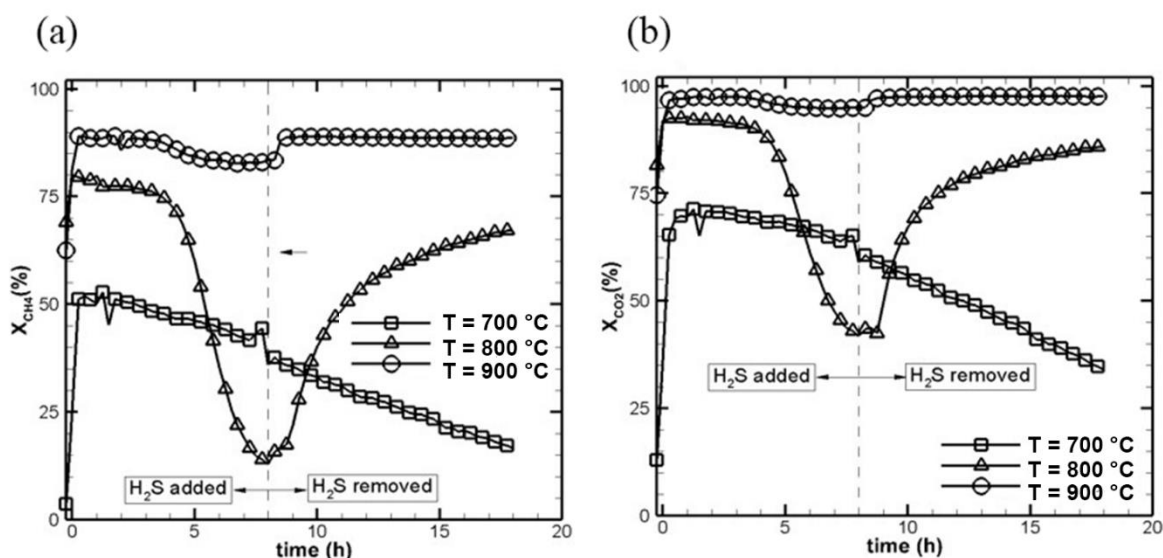


Figure 7. Effect of the reaction temperature on catalyst regeneration. CH₄/CO₂ = 1. (a) CH₄ conversion and (b) CO₂ conversion.

In Figure 8, the result of the poisoned catalyst regeneration under the O_{2999} treatment is shown. During this process, the surface-adsorbed sulfur may be oxidized, and the Ni sites are recovered back to NiO:

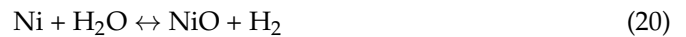


With the introduction of H_2 gas flow for two h, NiO is reduced into the active Ni sites. It is seen by using the regenerated catalyst that X_{CH_4} and X_{CO_2} increase with the increased test time and approach to constant values that can result, as shown in Figure 2. This indicated that the sulfur can be almost completely removed by the formation of SO_2 based on Equation (16). It was pointed out by Li et al. [41] that $NiSO_4$ is formed instead of SO_2 when a high O_2 flow was used based on the reaction



In this case, the catalyst would lose its activity in the DRM.

Similar to the O_2 treatment, the steam treatment for poisoned catalyst regeneration used the steam flow instead of the O_2 flow. The steam treatment removes sulfur in the form of SO_2 and H_2S and oxidizes Ni to NiO via the following reactions [42]:



By introducing a H_2 gas flow for two h, NiO is reduced into the active Ni sites. In Figure 9, the performance of the steam-regenerated catalyst is shown. It is seen that a certain amount of sulfur absorbed on the catalyst is not effectively removed during the regeneration treatment. This may be due to the relatively short time of the steam treatment. As a result, decreases in both X_{CH_4} and X_{CO_2} were observed by using the partially regenerated catalyst.

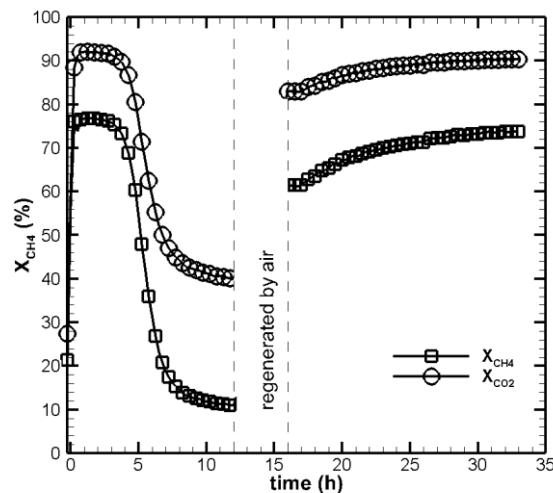


Figure 8. Poisoned catalyst regeneration using the high-temperature oxidation treatment. $T = 800\text{ }^\circ\text{C}$ and $CH_4/CO_2 = 1$. The catalyst was poisoned from 0 to 12 h, regenerated by 10-sccm air from 12 to 14 h to form NiO, reduced NiO to Ni by 20-sccm H_2 from 14 to 16 h, and DRM-tested using the regenerated catalyst from 16 to 33 h.

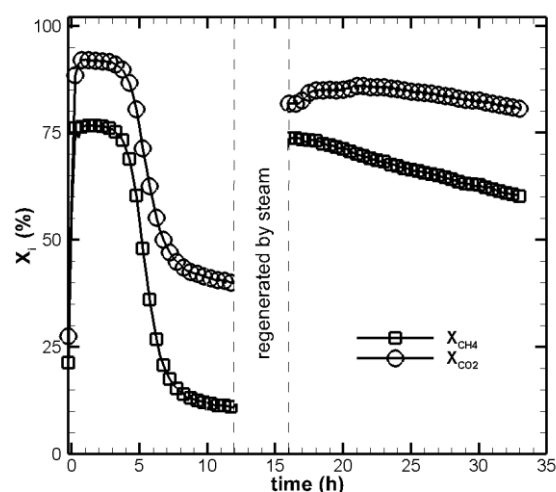


Figure 9. Poisoned catalyst regeneration using steam. $T = 800\text{ }^{\circ}\text{C}$ and $\text{CH}_4/\text{CO}_2 = 1$. The catalyst was poisoned from 0 to 12 h, regenerated by 10-sccm oxygen from 12 to 14 h to form NiO, reduced NiO to Ni by 20-sccm H_2 from 14 to 16 h, and DRM-tested using the regenerated catalyst from 16 to 33 h.

5. Conclusions

In this study, the performance of DRM using biogas as a feedstock was studied, including the catalyst poison, by the presence of H_2S in the reactant. Using the nonpoisoned DRM performance as a comparison basis, the following conclusions can be made:

- (1) The catalyst poison depends on both the reaction temperature and time. The H_2S coverage onto the catalyst surface decreases with the increased reaction temperature.
- (2) Due to the stronger chemisorption of sulfur onto the catalyst as compared to O_2 or H_2O , catalyst deactivation cannot be regenerated by the bi-reforming of methane in which DRM is combined with POM, COM, or SRM.
- (3) The catalyst cannot be regenerated for the poison that occurs at low temperatures.
- (4) The poisoned catalyst can be effectively regenerated using a high-temperature oxidation process. A higher reaction time is required for the catalyst regenerated by the high-temperature steam process.

Author Contributions: R.-Y.C. created the research concept, performed the experiments, analyzed data, and wrote the paper. Y.-C.C. performed the experiments and collected and analyzed the data. W.-H.C. organized the work, designed the experiments, analyzed data, and wrote the paper. All authors have read and agreed to the published version of the manuscript.

Funding: This research was funded by the Ministry of Science and Technology, Taiwan, R.O.C., under the contracts MOST 108-2221-E-006-127-MY3 and MOST 109-2622-E-006-006-CC1.

Data Availability Statement: Not applicable.

Acknowledgments: The authors acknowledge the financial support of the Ministry of Science and Technology, Taiwan, R.O.C., under the contracts MOST 108-2221-E-006-127-MY3 and MOST 109-2622-E-006-006-CC1 for this research.

Conflicts of Interest: The authors declare no conflict of interest.

References

1. Sadhwani, N.; Adhikari, S.; Eden, M. Biomass Gasification Using Carbon Dioxide: Effect of Temperature, CO_2/C Ratio, and the Study of Reactions Influencing the Process. *Ind. Eng. Chem. Res.* **2016**, *55*, 2883–2891. [[CrossRef](#)]
2. Chen, W.-H.; Lin, S.-C. Biogas partial oxidation in a heat recirculation reactor for syngas production and CO_2 utilization. *Appl. Energy* **2018**, *217*, 113–125. [[CrossRef](#)]
3. Hernández, B.; Martín, M. Optimal Process Operation for Biogas Reforming to Methanol: Effects of Dry Reforming and Biogas Composition. *Ind. Eng. Chem. Res.* **2016**, *55*, 6677–6685. [[CrossRef](#)]

4. Kang, J.Y.; Kang, D.W.; Kim, T.S.; Hur, K.B. Comparative economic analysis of gas turbine-based power generation and combined heat and power systems using biogas fuel. *Energy* **2014**, *67*, 309–318. [[CrossRef](#)]
5. Tamoor, M.; Tahir, M.S.; Sagir, M.; Iqbal, S.; Nawaz, T. Design of 3 kW integrated power generation system from solar and biogas. *Int. J. Hydrogen Energy* **2020**, *45*, 12711–12720. [[CrossRef](#)]
6. Gao, Y.; Jiang, J.; Meng, Y.; Yan, F.; Aihemaiti, A. A review of recent developments in hydrogen production via biogas dry reforming. *Energy Convers. Manag.* **2018**, *171*, 133–155. [[CrossRef](#)]
7. Zhao, X.; Joseph, B.; Kuhn, J.; Ozcan, S. Biogas Reforming to Syngas: A Review. *iScience* **2020**, *23*, 101082. [[CrossRef](#)] [[PubMed](#)]
8. Jung, S.; Lee, J.; Moon, D.H.; Kim, K.-H.; Kwon, E.E. Upgrading biogas into syngas through dry reforming. *Renew. Sustain. Energy Rev.* **2021**, *143*, 110949. [[CrossRef](#)]
9. Chen, W.-H.; Lin, M.-R.; Lu, J.-J.; Chao, Y.; Leu, T.-S. Thermodynamic analysis of hydrogen production from methane via autothermal reforming and partial oxidation followed by water gas shift reaction. *Int. J. Hydrogen Energy* **2010**, *35*, 11787–11797. [[CrossRef](#)]
10. Cañete, B.; Gigola, C.E.; Brignole, N.B. Synthesis Gas Processes for Methanol Production via CH₄ Reforming with CO₂, H₂O, and O₂. *Ind. Eng. Chem. Res.* **2014**, *53*, 7103–7112. [[CrossRef](#)]
11. James, O.O.; Mesubi, A.M.; Ako, T.C.; Maity, S. Increasing carbon utilization in Fischer–Tropsch synthesis using H₂-deficient or CO₂-rich syngas feeds. *Fuel Process. Technol.* **2010**, *91*, 136–144. [[CrossRef](#)]
12. Wang, C.; Wang, Y.; Chen, M.; Liang, D.; Yang, Z.; Cheng, W.; Tang, Z.; Wang, J.; Zhang, H. Recent advances during CH₄ dry reforming for syngas production: A mini review. *Int. J. Hydrogen Energy* **2021**, *46*, 5852–5874. [[CrossRef](#)]
13. Argyle, M.D.; Bartholomew, C.H. Heterogeneous Catalyst Deactivation and Regeneration: A Review. *Catalysts* **2015**, *5*, 145. [[CrossRef](#)]
14. Meloni, E.; Martino, M.; Palma, V. A Short Review on Ni Based Catalysts and Related Engineering Issues for Methane Steam Reforming. *Catalysts* **2020**, *10*, 352. [[CrossRef](#)]
15. Chein, R.; Yang, Z. H₂S effect on dry reforming of biogas for syngas production. *Int. J. Energy Res.* **2019**, *43*, 3330–3345. [[CrossRef](#)]
16. Jablonski, W.S.; Villano, S.M.; Dean, A.M. A comparison of H₂S, SO₂, and COS poisoning on Ni/YSZ and Ni/K₂O-CaAl₂O₄ during methane steam and dry reforming. *Appl. Catal. A Gen.* **2015**, *502*, 399–409. [[CrossRef](#)]
17. Rostrup-Nielsen, J.; Christiansen, L.J. *Concepts in Syngas Manufacture*; World Scientific: Singapore, 2011.
18. Izquierdo, U.; García-García, I.; Gutierrez, Á.M.; Arraibi, J.R.; Barrio, V.L.; Cambra, J.F.; Arias, P.L. Catalyst Deactivation and Regeneration Processes in Biogas Tri-Reforming Process. The Effect of Hydrogen Sulfide Addition. *Catalysts* **2018**, *8*, 12. [[CrossRef](#)]
19. Wachter, P.; Gaber, C.; Raic, J.; Demuth, M.; Hochenauer, C. Experimental investigation on H₂S and SO₂ sulphur poisoning and regeneration of a commercially available Ni-catalyst during methane tri-reforming. *Int. J. Hydrogen Energy* **2021**, *46*, 3437–3452. [[CrossRef](#)]
20. Wang, S.; Lu, G.Q.; Millar, G.J. Carbon Dioxide Reforming of Methane To Produce Synthesis Gas over Metal-Supported Catalysts: State of the Art. *Energy Fuels* **1996**, *10*, 896–904. [[CrossRef](#)]
21. Chen, W.-H.; Chen, C.-Y. Water gas shift reaction for hydrogen production and carbon dioxide capture: A review. *Appl. Energy* **2020**, *258*, 114078. [[CrossRef](#)]
22. Fidalgo, B.; Muradov, N.; Menéndez, J.A. Effect of H₂S on carbon-catalyzed methane decomposition and CO₂ reforming reactions. *Int. J. Hydrogen Energy* **2012**, *37*, 14187–14194. [[CrossRef](#)]
23. Rostrup-Nielsen, J.R. New aspects of syngas production and use. *Catal. Today* **2000**, *63*, 159–164. [[CrossRef](#)]
24. Bartholomew, C.; Agrawal, P.; Katzer, J. Sulfur Poisoning of Metals. *Adv. Catal.* **1982**, *31*, 135–242.
25. Chein, R.-Y.; Fung, W.-Y. Syngas production via dry reforming of methane over CeO₂ modified Ni/Al₂O₃ catalysts. *Int. J. Hydrogen Energy* **2019**, *44*, 14303–14315. [[CrossRef](#)]
26. Ashrafi, M.; Pfeifer, C.; Pröll, T.; Hofbauer, H. Experimental Study of Model Biogas Catalytic Steam Reforming: 2. Impact of Sulfur on the Deactivation and Regeneration of Ni-Based Catalysts. *Energy Fuels* **2008**, *22*, 4190–4195. [[CrossRef](#)]
27. Yang, X. An experimental investigation on the deactivation and regeneration of a steam reforming catalyst. *Renew. Energy* **2017**, *112*, 17–24. [[CrossRef](#)]
28. Chen, X.; Jiang, J.; Yan, F.; Li, K.; Tian, S.; Gao, Y.; Zhou, H. Dry Reforming of Model Biogas on a Ni/SiO₂ Catalyst: Overall Performance and Mechanisms of Sulfur Poisoning and Regeneration. *ACS Sustain. Chem. Eng.* **2017**, *5*, 10248–10257. [[CrossRef](#)]
29. Kalai, D.Y.; Stangeland, K.; Tucho, W.M.; Jin, Y.; Yu, Z. Biogas reforming on hydrotalcite-derived Ni-Mg-Al catalysts: The effect of Ni loading and Ce promotion. *J. CO₂ Util.* **2019**, *33*, 189–200. [[CrossRef](#)]
30. Niu, J.; Liland, S.E.; Yang, J.; Rout, K.R.; Ran, J.; Chen, D. Effect of oxide additives on the hydrotalcite derived Ni catalysts for CO₂ reforming of methane. *Chem. Eng. J.* **2019**, *377*, 119763. [[CrossRef](#)]
31. Newnham, J.; Mantri, K.; Amin, M.H.; Tardio, J.; Bhargava, S.K. Highly stable and active Ni-mesoporous alumina catalysts for dry reforming of methane. *Int. J. Hydrogen Energy* **2012**, *37*, 1454–1464. [[CrossRef](#)]
32. Appari, S.; Janardhanan, V.M.; Bauri, R.; Jayanti, S. Deactivation and regeneration of Ni catalyst during steam reforming of model biogas: An experimental investigation. *Int. J. Hydrogen Energy* **2014**, *39*, 297–304. [[CrossRef](#)]
33. Chattanathan, S.A.; Adhikari, S.; McVey, M.; Fasina, O. Hydrogen production from biogas reforming and the effect of H₂S on CH₄ conversion. *Int. J. Hydrogen Energy* **2014**, *39*, 19905–19911. [[CrossRef](#)]

34. Dou, X.; Veksha, A.; Chan, W.P.; Oh, W.-D.; Liang, Y.N.; Teoh, F.; Mohamed, D.K.B.; Giannis, A.; Lisak, G.; Lim, T.-T. Poisoning effects of H₂S and HCl on the naphthalene steam reforming and water-gas shift activities of Ni and Fe catalysts. *Fuel* **2019**, *241*, 1008–1018. [[CrossRef](#)]
35. Chein, R.; Chen, Y.; Yu, C.; Chung, J. Thermodynamic analysis of dry reforming of CH₄ with CO₂ at high pressures. *J. Nat. Gas Sci. Eng.* **2015**, *26*, 617–629. [[CrossRef](#)]
36. Nikoo, M.K.; Amin, N. Thermodynamic analysis of carbon dioxide reforming of methane in view of solid carbon formation. *Fuel Process. Technol.* **2011**, *92*, 678–691. [[CrossRef](#)]
37. Kumar, N.; Shojaee, M.; Spivey, J. Catalytic bi-reforming of methane: From greenhouse gases to syngas. *Curr. Opin. Chem. Eng.* **2015**, *9*, 8–15. [[CrossRef](#)]
38. Olah, G.A.; Goepfert, A.; Czaun, M.; Prakash, G.K.S. Bi-reforming of Methane from Any Source with Steam and Carbon Dioxide Exclusively to Metgas (CO–2H₂) for Methanol and Hydrocarbon Synthesis. *J. Am. Chem. Soc.* **2013**, *135*, 648–650. [[CrossRef](#)]
39. Pawar, V.; Appari, S.; Monder, D.S.; Janardhanan, V.M. Study of the Combined Deactivation Due to Sulfur Poisoning and Carbon Deposition during Biogas Dry Reforming on Supported Ni Catalyst. *Ind. Eng. Chem. Res.* **2017**, *56*, 8448–8455. [[CrossRef](#)]
40. Sehested, J. Four challenges for nickel steam-reforming catalysts. *Catal. Today* **2006**, *111*, 103–110. [[CrossRef](#)]
41. Li, L.; Howard, C.; King, D.L.; Gerber, M.; Dagle, R.; Stevens, D. Regeneration of Sulfur Deactivated Ni-Based Biomass Syngas Cleaning Catalysts. *Ind. Eng. Chem. Res.* **2010**, *49*, 10144–10148. [[CrossRef](#)]
42. Lombard, C.; Ledoze, S.; Marencaq, E.; Marquaire, P.; Lenoc, D.; Bertrand, G.; Lopicque, F. In situ regeneration of the Ni-based catalytic reformer of a 5kW PEMFC system. *Int. J. Hydrogen Energy* **2006**, *31*, 437–440. [[CrossRef](#)]